

## Influence of nonlocal electrodynamics on the anisotropic vortex pinning in $\text{YNi}_2\text{B}_2\text{C}$

A. V. Silhanek,<sup>1</sup> J. R. Thompson,<sup>2</sup> L. Civale,<sup>1</sup> D. McK. Paul,<sup>3</sup> and C. V. Tomy<sup>3</sup>

<sup>1</sup>Comisión Nacional de Energía Atómica—Centro Atómico Bariloche and Instituto Balseiro, 8400 Bariloche, Argentina

<sup>2</sup>Oak Ridge National Laboratory, Oak Ridge, Tennessee 37831-6061

and Department of Physics, University of Tennessee, Knoxville, Tennessee 37996-1200

<sup>3</sup>Department of Physics, I.I.T. Powai, Mumbai 400076, India

(Received 5 February 2001; published 15 June 2001)

We have studied the pinning force density  $F_p$  of  $\text{YNi}_2\text{B}_2\text{C}$  superconductors for various field orientations. We observe anisotropies both between the  $c$  axis and the basal plane and within the plane that cannot be explained by the usual mass anisotropy. For magnetic field  $\mathbf{H}\parallel c$ , the reorientation structural transition in the vortex lattice due to nonlocality, which occurs at a field  $H_1\sim 1$  kOe, manifests itself as a kink in  $F_p(H)$ . When  $\mathbf{H}\perp c$ ,  $F_p$  is much larger and has a quite different  $H$  dependence, indicating that other pinning mechanisms are present. In this case the signature of nonlocal effects is the presence of a fourfold periodicity of  $F_p$  within the basal plane.

DOI: 10.1103/PhysRevB.64.012512

PACS number(s): 74.60.Ge, 74.60.Jg

After Kogan and co-workers<sup>1</sup> showed in 1996 that nonlocal electrodynamics effects are relevant in high- $\kappa$  superconductors in a broad  $H$ - $T$  domain, several works demonstrated that nonlocality gives rise to unusual properties of the vortex matter. Those studies were done mainly on the family of compounds  $R\text{Ni}_2\text{B}_2\text{C}$ , where  $R=\text{Lu},\text{Y},\text{Tm},\text{Er},\text{Ho},\text{Dy}$ . These borocarbides are very well suited to studying nonlocal effects due to their intermediate  $\kappa$  values ( $\sim 10$ – $20$ ), which result in a wide field range where the extended London description holds, their high transition temperature  $T_c$ , and the possibility of fabricating clean single crystals with a large electronic mean free path. Deviations of the equilibrium magnetization from the local London prediction,<sup>2</sup> structural phase transitions separating a variety of exotic rhombic and square flux line lattices (FLL's),<sup>3–10</sup> and fourfold anisotropies in the basal plane of these tetragonal materials<sup>11,12</sup> provide strong support for the nonlocal scenario.

Although the consequences of nonlocality on the equilibrium properties of the superconducting vortex matter is by now convincingly established, very little is known about its effects on the nonequilibrium vortex response. For both  $\text{YNi}_2\text{B}_2\text{C}$  and  $\text{LuNi}_2\text{B}_2\text{C}$ , Eskildsen *et al.*<sup>13</sup> have shown that, for  $\mathbf{H}\parallel c$  axis and well above the field  $H_2\sim 1$  kOe marking the transition from a rhombic to a square vortex lattice, the pinning properties sharply disagree with the expectations of the Larkin-Ovchinnikov collective pinning theory for a triangular lattice. The authors associated the discrepancy with the different (and to a large extent unknown) elastic properties of the square lattice. However, neither the irreversible response in other field orientations, where the lattice geometry is different, nor the influence of the lattice transitions themselves on vortex pinning have been experimentally explored until now. It is clear that vortex pinning, which involves distortions from equilibrium vortex configurations, should be affected by the symmetry changes in the lattice.

In this work we report a study of nonlocal effects on the vortex pinning of a single crystal of  $\text{YNi}_2\text{B}_2\text{C}$ . For  $\mathbf{H}\parallel c$  axis the field dependence of the pinning force density  $F_p$  exhibits a distinct kink at a field  $H^*$  that coincides with the first order

reorientation transition in the vortex lattice. The angular dependence of  $H^*$  (for  $\mathbf{H}$  inclined up to  $30^\circ$  from  $c$ ) provide further support for the association of the kink with the FLL transition. For  $\mathbf{H}$  in the  $ab$  plane,  $F_p$  is an order of magnitude larger and the field dependence is quite different. We discuss the possible origin of this anisotropy. Finally, we observe fourfold oscillations in the angular dependence of  $F_p$  in the basal plane, which also arise from nonlocal effects.

The single crystal measured in the present study, with a mass of 17 mg, dimensions  $\sim 2\times 2.5\times 0.5$  mm, and critical temperature  $T_c=14.5$  K, is the same one used in previous work.<sup>2,11</sup> Electrical resistivity data yielded a residual resistance ratio of 10 and an estimate of the electronic mean free path  $l\sim 300$  Å. Magnetic measurements were carried out in two Quantum Design superconducting quantum interference device magnetometers. All data were taken in an MPMS-7 ( $H\leq 7$  T) except the angular dependence in the basal plane, which was studied in an MPMS-5S ( $H\leq 5$  T) using a home-made rotating system.<sup>14</sup> In the superconducting mixed state, isothermal magnetization loops were recorded. The hysteresis width  $\Delta M(H)$  was used to calculate the critical current density  $J_c$  from the Bean critical state model.

Figure 1(a) shows the pinning force density  $\mathbf{F}_p=\mathbf{J}_c\times\mathbf{B}$  as a function of  $\mathbf{H}\parallel c$  axis at several temperatures. At  $T=3$  K, after an initial increase at very low  $H$  (not shown),  $F_p(H)$  maximizes at a remarkably low reduced field ( $H/H_{c2}<0.01$ ), and then decreases approximately linearly in  $\log H$ . At a field  $H^*\sim 1$  kOe a clear kink is observed. Above this field  $F_p$  is still linear in  $\log H$ , but the slope  $dF_p/d\log H$  is smaller. At a higher field  $H_b\sim 10$  kOe a small bump is visible. As discussed below, we associate  $H_b$  with the peak observed by Eskildsen *et al.*<sup>13</sup> in  $\text{LuNi}_2\text{B}_2\text{C}$ . Finally, close to  $H_{c2}$  we observe the peak effect attributed to the softening of the FLL.

According to Kogan *et al.*'s model,<sup>4</sup> for  $\mathbf{H}\parallel c$  two structural transitions in the FLL occur in  $\text{YNi}_2\text{B}_2\text{C}$ , namely, a first order reorientation transition between two rhombic lattices at a field  $H_1$  and a second order transition from the rhombic to a square lattice at a higher field  $H_2$ . Recent calculations by

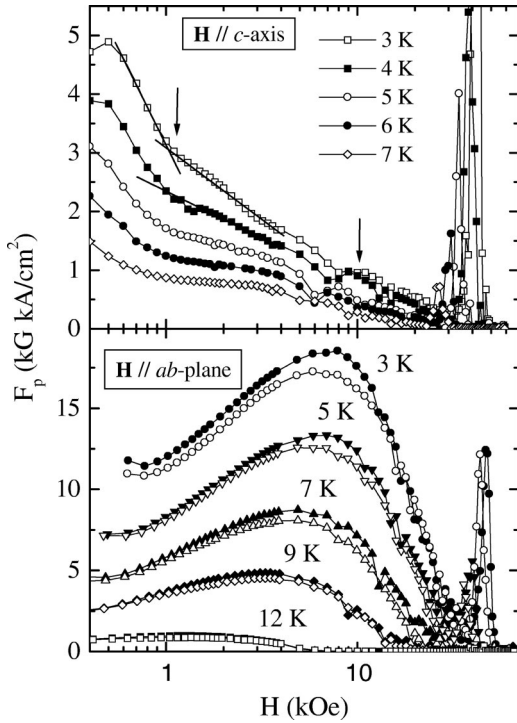


FIG. 1. Pinning force density  $F_p$  vs  $H$  for  $\text{YNi}_2\text{B}_2\text{C}$  single crystal with (a)  $\mathbf{H} \parallel c$  axis and (b)  $\mathbf{H} \parallel [100]$  (solid symbols) and  $\mathbf{H} \parallel [110]$  (open symbols) at several temperatures.

Knigavko *et al.*<sup>15</sup> show that the reorientation at  $H_1$  really consists of two second order transitions, but they take place in such a narrow field range that it may be hard to resolve them experimentally. Small angle neutron scattering (SANS) experiments<sup>8</sup> (performed on a crystal of the same batch as ours) confirmed Kogan *et al.*'s predictions. A jump in the apical angle  $\beta$  of the rhombic FLL (discontinuous within the resolution) occurs at  $H_1 \sim 1-1.25$  kOe, and the lattice becomes square ( $\beta=90^\circ$ ) at  $H_2 \sim 1.25-1.5$  kOe. The coincidence of our  $H^*$  with this field range makes it tempting to associate the jump in  $dF_p/d \log H$  with one of these transitions. However, the small difference between  $H_1$  and  $H_2$  makes it difficult to determine which one of them.

To solve this question we need to modify the experimental conditions in such a way that  $H_1$  and  $H_2$  change and split apart. The simplest way is to change  $T$ . Figure 1(a) shows that as  $T$  increases  $H^*$  remains almost constant, while the slope change progressively washes out. This last observation is consistent with the association of  $H^*$  with nonlocality, as those effects tend to disappear as  $T$  approaches  $T_c$ . On the other hand, theoretical expectations<sup>4</sup> as well as some qualitative experimental evidence<sup>5</sup> suggest that  $H_2$  increases with  $T$  well below  $T_c$ , in contrast with the observed behavior of  $H^*$ . This seems to indicate that the kink is not related to  $H_2$ .

To our knowledge there are no experimental data on the temperature dependence of  $H_1$ . The only theoretical hint comes from the recent study of Knigavko *et al.*<sup>15</sup> It is shown there that  $H_1$  in units of the scaling field  $\Phi_0/(2\pi\lambda)^2$  is a decreasing function of the strength of the nonlocal effects (which are parametrized by two averages over the Fermi surface,  $n$  and  $d$ ), and consequently must increase with  $T$ . Dis-

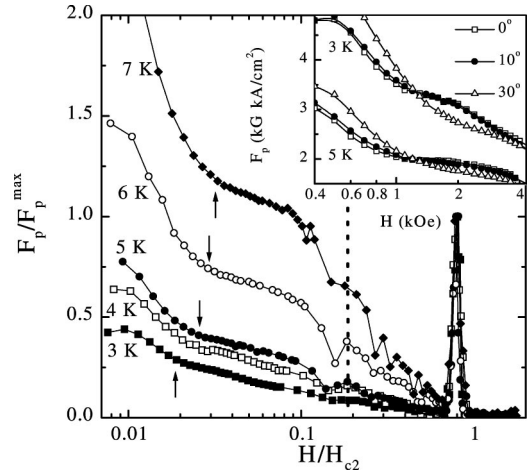


FIG. 2. Reduced pinning force density  $F_p/F_p^{\max}$  vs  $H/H_{c2}$  at several temperatures with  $\mathbf{H} \parallel c$  axis. The inset shows  $F_p$  versus  $H$  for  $\mathbf{H} \parallel c$  ( $\Theta=0^\circ$ ) and tilted  $10^\circ$  and  $30^\circ$  from  $c$ .

regarding a weak temperature dependence in  $\kappa$ , the scaling field is proportional to  $H_{c2}$ , which is easily accessed experimentally. This suggests analyzing  $F_p$  as a function of the reduced field  $h=H/H_{c2}$ .

In Fig. 2 we replotted the data of Fig. 1(a) as  $f_p = F_p/F_p^{\text{peak}}$  vs  $h$ . Here  $F_p^{\text{peak}}$  is the maximum of  $F_p$  at the peak close to  $H_{c2}$ , which occurs at the same reduced field  $h_p=0.8$  for all  $T$ . The overlap of the data at different  $T$  in the  $h$  range of the peak effect means that the pinning mechanism responsible for it satisfies a scaling law  $F_p(H,T) = F_p^{\text{peak}}(T)f_p(h)$ , as seen in many systems.<sup>16</sup> On the other hand, the fact that at lower  $h$  the  $f_p(h)$  data at various  $T$  do not collapse on a single curve indicates that the dominant pinning mechanism(s) in that range is (are) different from that originating the peak effect. As already mentioned, we identify the bump at intermediate field with the peak reported by Eskildsen *et al.*<sup>13</sup> The fact that this bump occurs at the same  $h_b \sim 0.18$  for all  $T$  is consistent with the interpretation of this feature as resulting from the stiffening of the vortex matter due to the increase of the shear modulus  $C_{66}$ , as this elastic constant depends on field only through  $h$ .<sup>13</sup>

In contrast to  $h_p$  and  $h_b$ , Fig. 2 shows that  $h^* = H^*/H_{c2}$  is temperature dependent. This lack of scaling is expected for features arising from nonlocal effects, as they involve the characteristic field  $H_0 \propto n^{-2}$ , whose  $T$  dependence is quite different from that of  $H_{c2}$ . In particular, the fact that  $h^*$  increases with  $T$  is consistent with the theoretical prediction for  $h_1 = H_1/H_{c2}$  as discussed above. So from the temperature dependence of  $H^*$  we conclude that it is probably associated with  $H_1$ .

Further evidence that  $H^*$  is a signature of the reorientation transition at  $H_1$  arises from the angular dependence. SANS results show<sup>8</sup> that  $H_2$  is very sensitive to the field orientation, while  $H_1$  is much less so. When  $\mathbf{H}$  is tilted by an angle  $\Theta = 10^\circ$  from the  $c$  axis,  $H_1$  remains unchanged within the resolution, while  $H_2$  shifts up significantly. Extrapolation of the data (the maximum measured field was 2.5 kOe) gives  $H_2 \sim 2.7$  kOe. For  $\Theta = 30^\circ$  only four SANS data points are available. Now  $\beta$  increases only weakly with  $H$ , and extrapo-

lation suggests that  $H_2$  is well above 4 kOe. The inset of Fig. 2 shows  $F_p$  vs  $\log H$  at  $T=3$  and 5 K, for  $\Theta=0^\circ$ ,  $10^\circ$ , and  $30^\circ$ . The  $10^\circ$  curves are almost identical to those for  $\mathbf{H}\parallel c$  and the kink is clearly visible at the same  $H^*$ , indicating that it is related to  $H_1$  rather than to  $H_2$ . In the  $\Theta=30^\circ$  curves  $H^*$  is slightly shifted up, while according to the SANS data  $H_1$  has either disappeared or shifted down to  $H<1$  kOe. However, the SANS evidence in this case is inconclusive, as it is based on a single data point and it may be affected by phase coexistence.

The very low  $J_c$  for  $\mathbf{H}\parallel c$  indicates that pinning correlation volumes are large, as confirmed by SANS results.<sup>13</sup> Thus, the elastic properties of the vortex lattice must play a key role in the pinning. While the tilt modulus  $C_{44} = BH/4\pi$  should be rather independent of the lattice details, it is easy to see that  $C_{66}$  depends on  $\beta$ . As  $\beta$  undergoes a discontinuous jump at  $H_1$ , it is natural to ascribe the kink to an abrupt change in  $C_{66}$ . It has been argued<sup>13</sup> that below  $H_b$  the collective pinning description is valid in  $\text{YNi}_2\text{B}_2\text{C}$ . In the simplest scenario this implies that  $F_p \propto C_{44}^{-1} C_{66}^{-2}$ . Using this expression and the experimental  $F_p(H)$  we computed  $C_{66}(H)$ , and indeed found a kink at  $H^*$  as expected. The surprising result is that  $C_{66}$  decreases monotonically with increasing  $H$  both below and above  $H^*$ , in contradiction with the standard behavior. It must be noted, however, that the shear properties for  $\beta \neq 60^\circ$  are anisotropic; thus  $C_{66}$  has more than one component and the expression for  $F_p$  should be modified.

We now turn to the pinning properties for  $\mathbf{H}\perp c$ . Figure 1(b) shows  $F_p(H)$  for  $\mathbf{H}\parallel[100]$  and  $\mathbf{H}\parallel[110]$  at various  $T$ . The behavior in these orientations is very different from that at  $\mathbf{H}\parallel c$ . At  $T=3$  K a broad maximum occurs at a field  $H_{max} \sim 7$  kOe. Over most of the field range  $F_p$  is much larger than for  $\mathbf{H}\parallel c$ , the maximum in this out-of-plane anisotropy being a factor of  $\sim 20$  at  $H_{max}$ . As  $T$  increases,  $H_{max}$  decreases while the anisotropy remains approximately constant. This large  $F_p$  anisotropy is surprising. Since the mass anisotropy<sup>12</sup> is very small ( $<10\%$ ) as confirmed by the  $H_{c2}$  values in Figs. 1(a) and 1(b), this behavior cannot be explained by the anisotropic scaling frequently used in high  $T_c$  superconductors.<sup>17</sup>

We have ruled out the existence of significant surface barriers (or pinning concentrated on the surface) for  $\mathbf{H}\perp c$ , by performing minor hysteresis loops for  $\mathbf{H}$  in the  $ab$  plane at several  $T$  and  $H$ . If hysteresis were due to surface barriers no flux changes would occur in the bulk while  $H$  is changing from one branch of the main loop to the other one; hence the data of the minor loop connecting the lower and upper branches would be<sup>18</sup> Meissner-like straight lines. In contrast, in the case of bulk pinning, the lines connecting the two branches are curved (parabolic in the simplest Bean model for an infinite slab) just as we observe in all cases. Moreover, the  $F_p$  values calculated from these minor loops are in good agreement with those shown in Fig. 1(b).

Another potential source of this anisotropic pinning is the small amount of magnetic impurities present in this crystal,<sup>11</sup> about  $\sim 0.1\%$  of a rare earth substituting for Y, whose moments lie in the basal plane. However, although we cannot

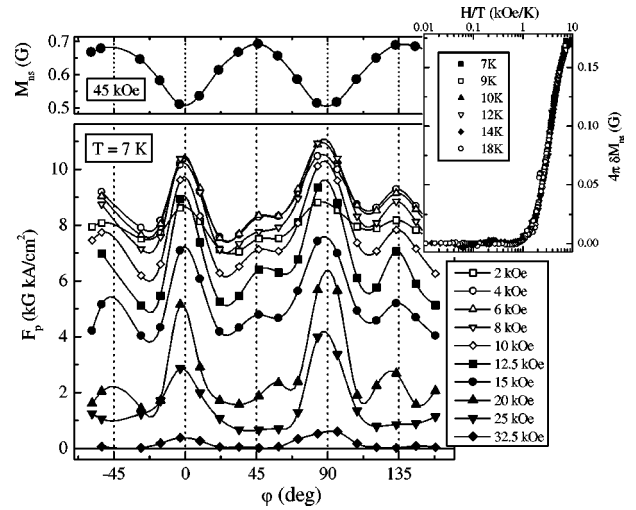


FIG. 3. Upper panel: the normal state magnetization  $M_{ns}$  at  $T=7$  K and  $H=45$  kOe, as a function of the angle  $\varphi$  between the applied field  $\mathbf{H}$  (contained in the  $ab$  basal plane) and the  $a$  axis. Lower panel: pinning force density  $F_p(\varphi)$  at  $T=7$  K and several fields. Inset: oscillation amplitude of the in-plane normal state magnetization,  $\delta M_{ns} = M_{ns}[110] - M_{ns}[100]$ , vs  $H/T$ .

totally rule out this possibility, the data suggest that this is not the case. As the localized moments' alignment increases with increasing  $H$ , the directional pinning efficiency, and thus the out-of-plane anisotropy in  $F_p$ , should increase monotonically with increasing  $H$ . On the contrary, at  $T=3$  K the anisotropy factor is already large ( $\sim 6$ ) at  $H \sim 1$  kOe, then it grows with  $H$ , maximizes at  $H_{max}$ , and decreases again for higher  $H$ . In particular,  $F_p$  is almost isotropic (within  $\sim 10\%$ ) in the peak effect.

In brief, the origin of the large out-of-plane anisotropy in  $F_p$  is unclear. It seems too large to be ascribed to nonlocality, which should appear as a perturbative effect. A simple explanation could be the presence of some still unidentified anisotropic pins, such as planar defects.

Another feature visible in Fig. 1(b) is the in-plane anisotropy,  $F_p[100] > F_p[110]$ . The difference is small but systematic. The fourfold nature of this in-plane anisotropy is clearly demonstrated by the data in the lower panel of Fig. 3, where the in-plane angular dependence of the pinning force density  $F_p(\varphi)$  at  $T=7$  K is shown for several  $H$ . The behavior of  $F_p(\varphi)$  is rather complex: in addition to the main peaks at  $[100]$  and  $[010]$ , secondary maxima are visible at  $[110]$  and  $[1\bar{1}0]$ .

We will now discuss the possible sources of this fourfold in-plane anisotropy. Of course mass anisotropy (a second rank tensor) cannot account for any angular dependence in the basal plane of this tetragonal compound. We can also discard artifacts due to misalignment between the  $c$  axis and the sample rotation axis, or to sample shape effects. A misalignment can only produce twofold oscillations, and the same is true for the shape effects if the sample geometry can be approximated by an ellipse. This is indeed the case in this crystal, and from the eccentricity of the ellipse the amplitude of the twofold oscillations can be estimated as  $\sim 2\%$ .<sup>11</sup> This small effect is in fact observed in Fig. 3, as



$F_p(\varphi=90^\circ)$  is systematically larger than  $F_p(\varphi=0^\circ)$ . Even if the small deviations from the elliptical shape were relevant, the nontrivial  $T$  and  $H$  dependence of  $F_p(\varphi)$  cannot be accounted for by a simple geometrical factor relating  $\Delta M$  and  $J_c$ .

Another possible source of the in-plane anisotropy is again the presence of magnetic impurities. However, the normal state magnetization  $M_{ns}$  shows that the Curie tail due to the localized moments is isotropic within the  $ab$  plane for values of the scaling variable  $H/T$  up to  $\sim 1$  kOe/K. For higher  $H/T$  a fourfold anisotropy appears. This is seen in the inset of Fig. 3, where  $\delta M_{ns} = M_{ns}[110] - M_{ns}[100]$  vs  $H/T$  is shown. Thus,  $F_p$  should be isotropic in the plane below the  $\sim 1$  kOe/K threshold. This is contrary to the results: Fig. 1(b) shows that at all  $T \leq 9$  K the in-plane anisotropy in  $F_p$  is already visible well below  $H/T \sim 1$  kOe/K. Similarly, Fig. 3 shows that at  $T=7$  K (where  $M_{ns}$  is isotropic up to  $\sim 7$  kOe) the fourfold oscillations in  $F_p$  occur for all  $H > 2$  kOe. Further evidence that the localized moments are not the source of the in-plane pinning anisotropy is that the oscillations in  $M_{ns}$  (shown in the upper panel of Fig. 3 for  $H=45$  kOe) and in  $F_p$  have opposite signs.

While it is very unlikely that any type of crystallographic defect could account for the complex four- and higher-fold in-plane variations in  $F_p$ , nonlocal effects can provide a natural explanation for them. Due to nonlocality, the geometry of the vortex lattice depends on the orientation within the plane. We can again argue (as in the  $\mathbf{H} \parallel c$  case) that  $C_{66}$

depends on the lattice geometry, and that such dependence must be reflected in  $F_p$ . Interestingly,  $F_p$  has local maxima at the high symmetry crystallographic orientations  $[100]$  and  $[110]$ , where  $C_{66}$  is expected to exhibit local minima. The fact that the in-plane anisotropy smoothly decreases as  $T$  approaches  $T_c$  provides further support to this interpretation.

In conclusion,  $F_p$  in  $\text{YNi}_2\text{B}_2\text{C}$  exhibits a rich anisotropic behavior that sharply contrasts with its small mass anisotropy. Nonlocal electrodynamics influences pinning via the unusual behavior of the shear modulus in nonhexagonal lattices, through either continuous variations (fourfold basal plane anisotropy) or abrupt jumps (the kink at  $H_1$ ). A complete understanding of the vortex irreversible response will require a deeper knowledge of the elastic properties of nonhexagonal lattices and the extension of the pinning models to those structures. Clearly, the complexity of the angular dependence of  $F_p$  involves other mechanisms besides nonlocality. In particular, the origin of the unexpected large out-of-plane pinning anisotropy deserves further investigation.

This work was partially supported by ANPCyT, Argentina, PICT 97 No.01120, and CONICET PIP 4207. The research was sponsored by the U.S. Department of Energy under Contract No. DE-AC05-00OR22725 with the Oak Ridge National Laboratory, managed by UT-Battelle, LLC. We thank Hyun Jeong Kim for her valuable help in conducting experiments. We acknowledge useful discussions with D. K. Christen, M. Yethiraj, and H. R. Kerchner. A.V.S. would like to thank CONICET for financial support.

<sup>1</sup>V.G. Kogan, A. Gurevich, J.H. Cho, D.C. Johnston, Ming Xu, J.R. Thompson, and A. Martynovich, Phys. Rev. B **54**, 12 386 (1996).

<sup>2</sup>K.J. Song, J.R. Thompson, M. Yethiraj, D.K. Christen, C.V. Tomy, and D.McK. Paul, Phys. Rev. B **59**, R6620 (1999).

<sup>3</sup>M. Yethiraj, D.McK. Paul, C.V. Tomy, and E.M. Forgan, Phys. Rev. Lett. **78**, 4849 (1997).

<sup>4</sup>V.G. Kogan, M. Bullock, B. Harmon, P. Miranović, Lj. Dobrosavljević-Grujić, P.L. Gammel, and D.J. Bishop, Phys. Rev. B **55**, R8693 (1997).

<sup>5</sup>M.R. Eskildsen, P.L. Gammel, B.P. Barber, U. Yaron, A.P. Ramirez, D.A. Huse, D.J. Bishop, C. Bolle, C.M. Lieber, S. Oxx, S. Sridhar, N.H. Andersen, K. Mortensen, and P. Canfield, Phys. Rev. Lett. **78**, 1968 (1997).

<sup>6</sup>Y. De Wilde, M. Iavarone, U. Welp, V. Metlushko, A.E. Koshelev, I. Aranson, G.W. Crabtree, and P.C. Canfield, Phys. Rev. Lett. **78**, 4273 (1997).

<sup>7</sup>M. Yethiraj, D.McK. Paul, C.V. Tomy, and J.R. Thompson, Phys. Rev. B **58**, R14 767 (1998).

<sup>8</sup>D.McK. Paul, C.V. Tomy, C.M. Aegerter, R. Cubitt, S.H. Lloyd, E.M. Forgan, S.L. Lee, and M. Yethiraj, Phys. Rev. Lett. **80**, 1517 (1998).

<sup>9</sup>P.L. Gammel, D.J. Bishop, M.R. Eskildsen, K. Mortensen, N.H. Andersen, P.C. Canfield, and V. Kogan, Phys. Rev. Lett. **82**, 4082 (1999).

<sup>10</sup>H. Sakata, M. Oosawa, K. Matsuba, N. Nishida, H. Takeya, and K. Hirata, Phys. Rev. Lett. **84**, 1583 (2000).

<sup>11</sup>L. Civale, A.V. Silhanek, J.R. Thompson, K.J. Song, C.V. Tomy, and D.McK. Paul, Phys. Rev. Lett. **83**, 3920 (1999).

<sup>12</sup>V.G. Kogan, S.L. Budko, P.C. Canfield, and P. Miranovic, Phys. Rev. B **60**, R12 577 (1999).

<sup>13</sup>M.R. Eskildsen, P.L. Gammel, B.P. Barber, A.P. Ramirez, D.J. Bishop, N.H. Andersen, K. Mortensen, C.A. Bolle, C.M. Lieber, and P.C. Canfield, Phys. Rev. Lett. **79**, 487 (1997).

<sup>14</sup>A.V. Silhanek, L. Civale, S. Candia, G. Nieva, G. Pasquini, and H. Lanza, Phys. Rev. B **59**, 13 620 (1999).

<sup>15</sup>A. Knigavko, V.G. Kogan, B. Rosenstein, and T.J. Yang, Phys. Rev. B **62**, 111 (2000).

<sup>16</sup>E.J. Kramer, J. Appl. Phys. **44**, 1360 (1973); D. Dew-Hughes, Philos. Mag. **30**, 293 (1974).

<sup>17</sup>G. Blatter, V.B. Geshkenbein, and A.I. Larkin, Phys. Rev. Lett. **68**, 875 (1992).

<sup>18</sup>H. Ullmaier, *Irreversible Properties of Type II Superconductors* (Springer-Verlag, Berlin, 1975), p. 124.